ACS APPLIED MATERIALS & INTERFACES

Research Article

www.acsami.org

Smart Fiber Membrane for pH-Induced Oil/Water Separation

Jin-Jin Li, Yin-Ning Zhou, and Zheng-Hong Luo*

Department of Chemical Engineering, School of Chemistry and Chemical Engineering, Shanghai Jiao Tong University, Shanghai 200240, P. R. China

Supporting Information

ABSTRACT: Wastewater contaminated with oil or organic compounds poses threats to the environment and humans. Efficient separation of oil and water are highly desired yet still challenging. This paper reports the fabrication of a smart fiber membrane by depositing pH-responsive copolymer fibers on a stainless steel mesh through electrospinning. The cost-effective precursor material poly(methyl methacrylate)-*block*-poly(4-vinylpyridine) (PMMA-*b*-P4VP) was synthesized using copper(0)-mediated reversible-deactivation radical polymerization. The pH-responsive P4VP and the underwater oleophilic/hydrophilic PMMA confer the as-prepared membrane with switchable surface wettability toward water and oil. The three-dimensional network structure of the fibers considerably strengthens the oil/water wetting property of the membrane, which is highly desirable in the separation of oil and water mixtures. The as-prepared fiber membrane accomplishes gravity-driven pH-controllable oil/water separations. Oil selectively passes through the membrane, whereas water remains at the initial state; after the membrane is wetted with acidic water (pH 3), a reverse separation is realized. Both separations are highly efficient, and the membrane also exhibits switchable wettability after numerous cycles of the separation process. This cost-effective and easily mass-produced smart fiber membrane with excellent oil-fouling repellency has significant potential in practical applications, such as water purification and oil recovery.

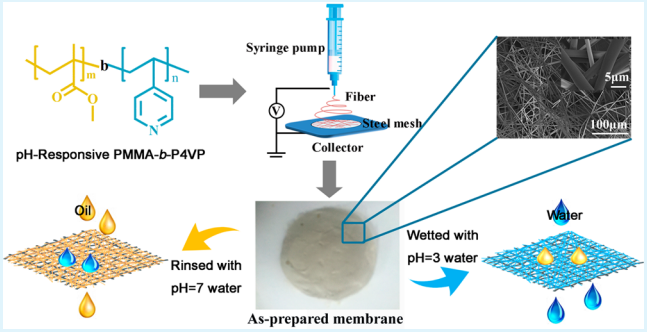

KEYWORDS: *electrospun fiber membrane, smart surface, pH-responsive, water wettability, oil wettability, oil/water separation*

1. INTRODUCTION

Industrial oily wastewater and oil spills pose threats to humans and the environment. Separating oily wastewater effectively has been a global challenge.[1−3] Interface science, especially with respect to the special wettability of a surface, provides solutions to these environmental issues.[4] A number of superwetting materials have been applied to oily wastewater separation through manipulation of both the surface structure and chemical composition.[5−17] In general, these separation materials are mainly classified into three types: "oil-removing",[5,6] "water-removing",[7,8] and smart controllable separation materials.[9−15] For smart materials, various external stimuli, such as thermal treatment,[9,10] light irradiation,[11] electrical field,[12] and pH,[13−15] have been employed to control the separation of oil/water mixtures. Smart materials with controllable oil/water wettability are promising for application to highly efficient oil/water separation, which requires simple separation devices and low energy use. Oil/water separation using such smart materials accounts for higher separation efficiency than oil/water separation using monofunctional materials.[16,17] Owing to the elaborate design, smart materials can switch their wettability toward both water and oil between two extreme states. For example, Zhang et al.[18] fabricated a smart surface based on a pH-responsive block copolymer for controllable oil/water separation and controllable capture/release of an oil droplet. However, the complex surface fabrication process may limit the practical applications of the fabricated smart surface.

Responsive copolymers with flexible and diversiform properties can be prepared using reversible-deactivation radical polymerization (RDRP) technologies, especially the copper(0)-mediated RDRP process, for ultrafast polymerization with small amounts of catalyst.[19,20] Polymer processing, being relatively low cost and easy, facilitates the large-area fabrication of functional surfaces. Thus, smart surfaces fabricated using responsive copolymers have gained considerable attention.[21,22] In addition to chemical composition, structural asperities as another important factor should be considered in constructing smart surfaces with special surface wettability.[23−28] The influence of roughness on the wetting behavior of a surface is explained by the Wenzel model[29] and the Cassie−Baxter model[30] (C−B model). The Wenzel model recognizes that the roughness can enhance both the wetting and antiwetting behaviors of the liquid on the surface. The C−B model indicates that the trapped air in the rough area can facilitate the construction of a super-antiwetting surface. In this aspect, electrospinning is a simple and low-cost method to construct polymeric surfaces with a special rough structure.[31−34] The

Received: May 13, 2015
Accepted: August 21, 2015
Published: August 21, 2015

DOI: 10.1021/acsami.5b04146
ACS Appl. Mater. Interfaces 2015, 7, 19643−19650

diameter of electrospun fibers can be regulated by the polymer solution concentration, polymer molecular weight, and applied voltage. Importantly, electrospun membranes consisting of continuous entangled fibers usually have a three-dimensional (3D) porous network structure and a high surface area-to-volume ratio, both of which make these membranes good candidates for oil/water separation.[31]

In this study, a simple method of electrospinning a pH-responsive copolymer poly(methyl methacrylate)-*block*-poly(4-vinylpyridine) (PMMA-*b*-P4VP) on a stainless steel mesh to fabricate a smart fiber membrane was carried out. The cost-effective precursor material PMMA-*b*-P4VP was precisely synthesized by employing copper(0)-mediated RDRP. In conjunction with the pH-responsiveness of P4VP and the underwater oleophilicity/hydrophilicity of PMMA, the 3D network structure of the fibers endowed the as-prepared membrane with two switchable wettability states (superhydrophobicity/superoleophilicity and superhydrophilicity/underwater superoleophobicity). As a consequence, the as-prepared fiber membrane accomplished gravity-driven pH-switchable oil/water separation. The relevant separation mechanism and the reversibility of the as-prepared membrane were investigated. This cost-effective and easily mass-produced smart fiber membrane with excellent antifouling properties against oil has considerable potential in practical applications, such as water purification and oil recovery.

2. EXPERIMENTAL SECTION

2.1. Materials. Methyl methacrylate [MMA; 98%, Sinopharm Chemical Reagent Co., Ltd. (SCRC)] was rinsed with an aqueous NaOH solution (5 wt %) to remove the inhibitor, dried with $MgSO_4$ overnight, and distilled before use. 4-Vinylpyridine (4VP, Acros, 96%) was passed through a basic alumina column in order to remove the inhibitor. Copper (wire, diameter 1.0 mm, 99.9%, Alfa Aesar) was typically washed with methanol/HCl first and then with methanol before use. Ethyl 2-bromoisobutyrate (Eib-Br, 98%, Alfa Aesar), hexamethylated tris(2-aminothyl)amine (Me_6-TREN, 99%, Alfa Aesar), and $CuCl_2$ (99%, Acros) were used as received. Dimethylformamide (DMF) and 2-propanol were obtained from SCRC and used without further purification. Other analytical reagents were used as received without further purification.

2.2. Synthesis of the Macroinitiator PMMA-Cl. A typical procedure to prepare chlorine end-capped PMMA (PMMA-Cl) was introduced as follows. A magnetic stirrer winded by activated copper(0) wire (diameter = 1.0 mm, 4 cm) and $CuCl_2$ (1.3 mg, 0.0094 mmol) were placed in the reaction flask, degassed, and filled with nitrogen three times. The deoxygenated solvent (DMF, 10 mL) and monomer MMA (15 mL, 141 mmol) previously bubbled by nitrogen for 30 min were then added to the flask. Last, Me_6-TREN (24 μL, 0.094 mmol) and the initiator (Eib-Br; 135.7 μL, 0.94 mmol) were added under a nitrogen flow. The reaction mixture was stirred in an oil bath with a thermostat at 50 °C. The reaction was terminated by quenching in liquid nitrogen at low conversion to keep high chain-end functionality. The resulting polymer was dissolved in chloroform, and the catalyst was removed by passing the polymer solution over an alumina column. The purified product was obtained through repeated precipitation from methanol and dried under vacuum.

2.3. Synthesis of PMMA-*b*-P4VP. PMMA-*b*-P4VP was synthesized by polymerization of 4VP using the previously reported copper(0) and a $CuCl_2$/Me_6-TREN = 1/1 catalytic system.[35,36] The detailed process was introduced as below. The macroinitiator PMMA-Cl (1.1 g, 0.12 mmol) was first dissolved in 6 mL of a DMF/2-propanol mixed solvent in a 2/1 volume ratio. A magnetic stirrer winded by activated copper(0) wire (diameter = 1.0 mm, 4 cm), $CuCl_2$ (8.1 mg, 0.06 mmol), and Me_6-TREN (15.3 μL, 0.06 mmol) were then placed in the reaction flask, and the system was deoxygenated with two freeze−vacuum−thaw cycles and purged with nitrogen. Last, 4VP (1.9 mL, 18 mmol) was added to the flask under a nitrogen flow, and the reaction mixture was deoxygenated through two freeze−vacuum−thaw cycles and purged with nitrogen again. Polymerization was performed at 50 °C for 7 h. The reaction solution was first diluted by chloroform, passed through an alumina column to remove the copper catalyst, and then deposited in cold ether. The obtained copolymer was dried in a vacuum oven at 50 °C.

2.4. Preparation of a Smart Fiber Membrane. PMMA-*b*-P4VP was first dissolved in chloroform/DMF in a 2/1 volume ratio to a concentration of 20 wt %. After stirring for 24, the prepared solution was electrospun in a closed chamber. During electrospinning, the applied voltage was kept at approximately 14 kV and the solution feeding rate was set at 0.2 mL/h through a syringe pump. The as-spun fibers were collected by the prepared stainless mesh, and the obtained fibrous membrane was dried in an air oven at 50 °C for 12 h to remove any residual solvent. Prior to electrospinning, stainless meshes (350 mesh size) were first cleaned by ethanol and acetone rinses and then tailored to a round shape with an area of 23.7 cm^2.

2.5. Instrumentation. ^{1}H NMR was recorded on a Varian Mercury Plus 400, 400 MHz NMR instrument. The molecular weights and molecular weight distributions (M_w/M_n) of the polymers were measured on a gel permeation chromatograph (Tosoh Corp.) equipped with two HLC-8320 columns (TSK gel Super AWM-H, pore size 9 μm, 6 × 150 mm, Tosoh Corp.) and a double-path, double-flow refractive index detector (Bryce) at 30 °C. Scanning electron microscopy (SEM) images of the fiber-coated films were obtained by a JEOL JSM-7500F scanning electron microscope. The contact-angles (CAs) of as-prepared fiber membrane surfaces were measured on a Contact Angle Measuring Instrument (KRUSS, DSA30). Please refer to the Supporting Information for details.

3. RESULTS AND DISCUSSION

3.1. Characterization of the Polymers. PMMA-*b*-P4VP was synthesized via sequential copper(0)-mediated RDRP, as described in Scheme 1. First, the macroinitiator chlorine end-capped PMMA (PMMA-Cl) was synthesized. Figure 1a shows the ^{1}H NMR spectra of the resulting polymers. In the red spectrum, the characteristic peaks 3.55−3.65 ppm (m, 3H, CH_3O−), 1.75−2.25 ppm (m, 2H, − CH_2CCH_3−), and 0.75−1.50 ppm (m, 3H, − CH_2CCH_3−) were clearly observed. In addition, the peak located at 4.00−4.20 ppm was attributed to the methylene protons (CH_3CH_2O−) of the organic initiator.

Scheme 1. Synthetic Outline of PMMA-Cl and PMMA-*b*-P4VP

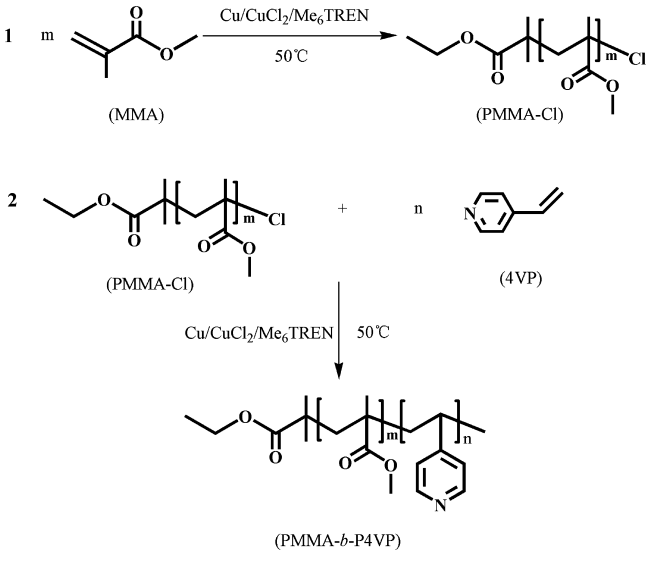

DOI: 10.1021/acsami.5b04146
ACS Appl. Mater. Interfaces 2015, 7, 19643−19650

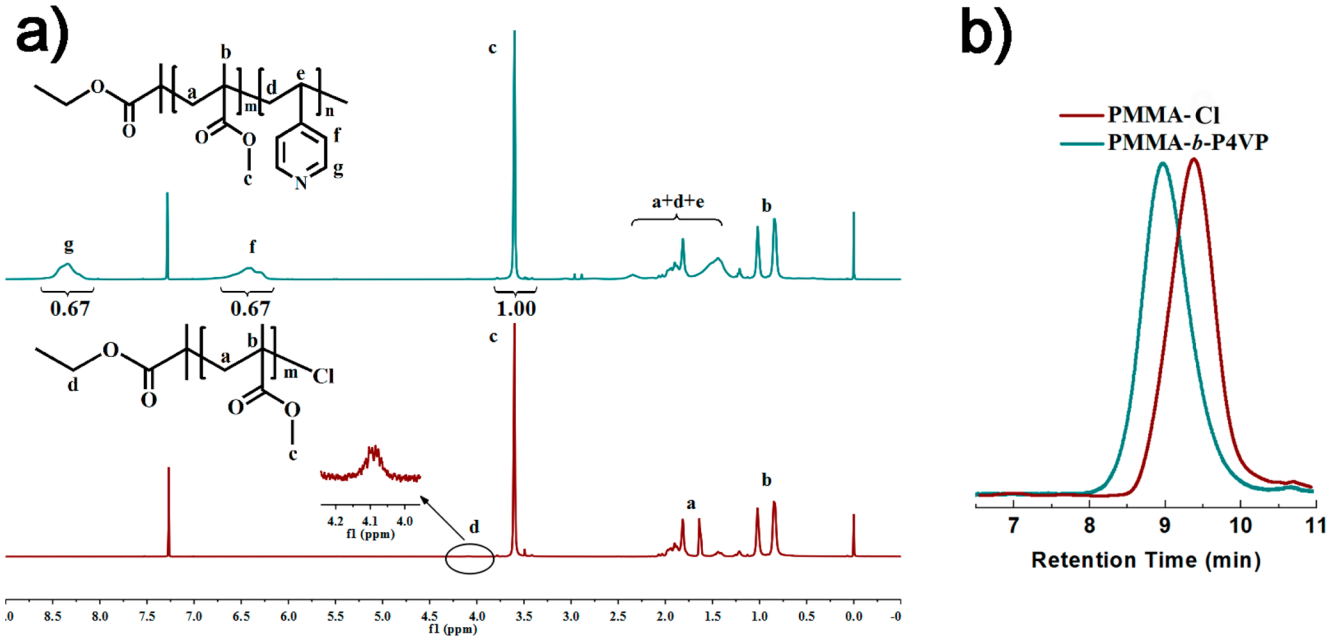

Figure 1. (a) ^{1}H NMR spectra and (b) GPC traces for PMMA-Cl (red line) and PMMA-*b*-P4VP (green line).

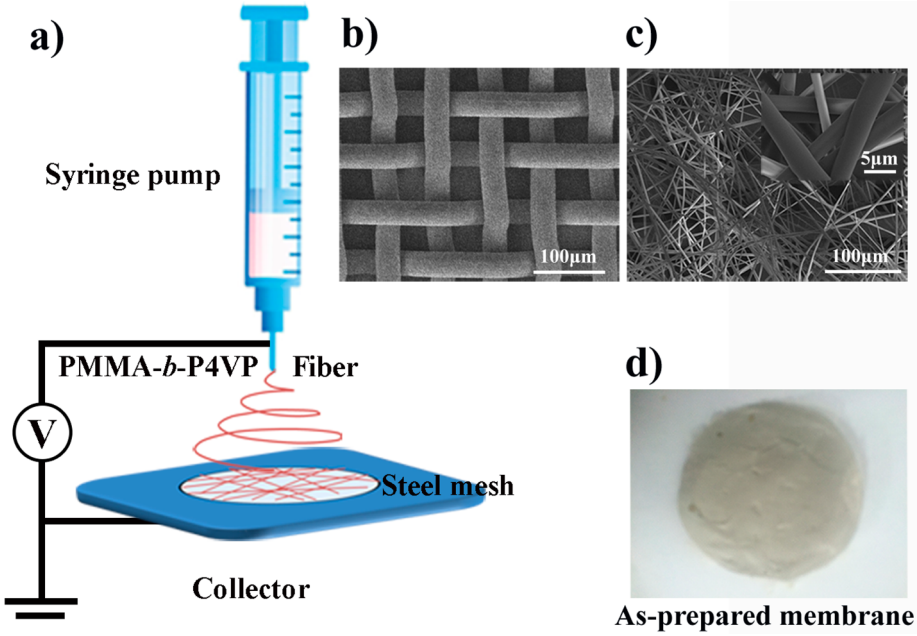

Figure 2. (a) Schematic showing the electrospun membrane fabrication process, (b) SEM image of the original stainless steel mesh, (c) SEM image of a fiber-coated stainless steel mesh with high and low magnification, and (d) photograph of the as-prepared PMMA-*b*-P4VP fiber membrane.

By comparing the integral area of methoxyl protons (CH_3O-, $A_{3.55-3.65}$) and that of CH_3CH_2O- protons ($A_{4.00-4.20}$), one can obtain the average polymerization degree (DP_n) of the macroinitiator. In this study, DP_n of PMMA-Cl is 82, which is denoted as a subscript in the succeeding paragraphs of this section. Therefore, M_n of $PMMA_{82}$-Cl is about 8200 g/mol.

Subsequently, the block copolymer PMMA-*b*-P4VP was prepared via the chain extension of $PMMA_{82}$-Cl. Notably, the polymerization of 4VP through conventional atom-transfer radical polymerization with the use of classical initiating/catalytic systems is challenging because both the 4VP monomer and P4VP can coordinate with a cupric salt catalyst. Besides, some side reactions (e.g., nucleophilic substitution, elimination reaction) can take place in conventional conditions.[35,36] Therefore, a carefully selected initiating/catalytic system was used in the present work. In this regard, a strong complexing ligand (Me_6-TREN) for the copper catalyst was used to effectively avoid complexation between the pyridine rings and the copper catalyst. $CuCl_2$ was used to obtain the chlorine end-capped macroinitiator and dormant species to eliminate the side reactions. The successful synthesis of a P4VP-containing block copolymer is supported by the ^{1}H NMR spectrum (Figure 1a, green line). The peaks at 6.20−6.80 and 8.10−8.60 ppm are assigned to the protons of the pyridine rings ($-CC_4H_4N$). Similarly, DP_n of P4VP was calculated by comparing the integral areas of $-CC_4H_4N$ protons

DOI: 10.1021/acsami.5b04146
ACS Appl. Mater. Interfaces 2015, 7, 19643−19650

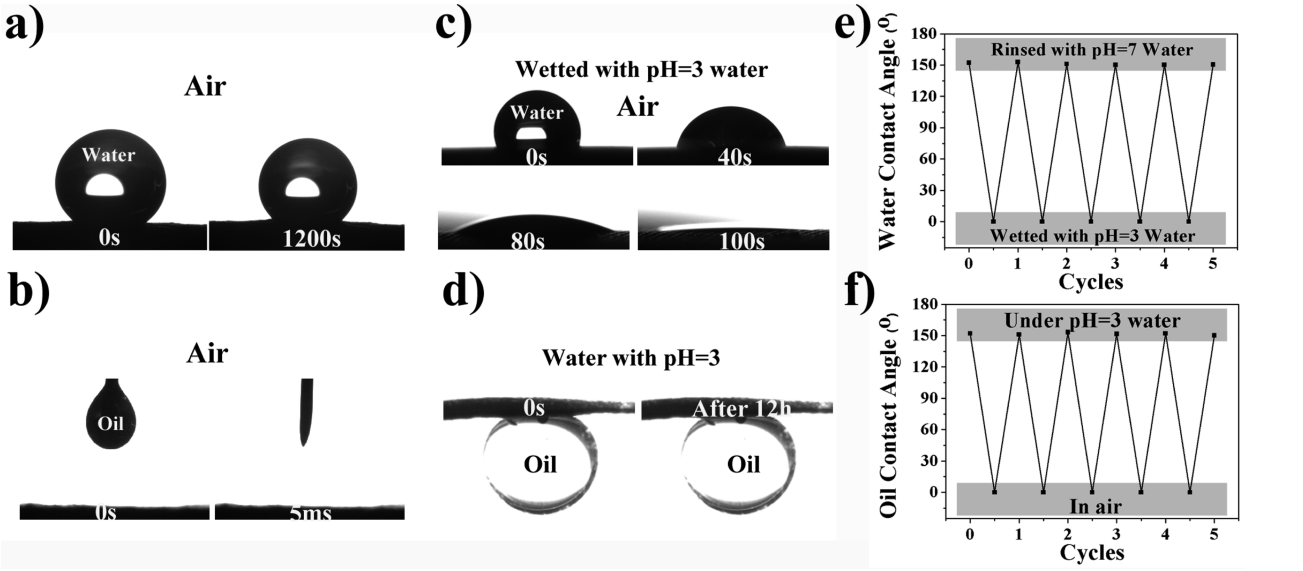

Figure 3. CA measurements of the as-prepared membrane: (a) images of a neutral water droplet on the as-prepared membrane at 0 s (left) and at 1200 s in air (right); (b) oil (*n*-hexane) droplet on the as-prepared membrane in air, for which *n*-hexane was quickly absorbed within 5 ms; (c) neutral water droplet on the membrane wetted with acidic water (pH 3) and slightly dried under a nitrogen flow, for which the droplet spread over the surface gradually within 100 s; (d) images of the oil (*n*-hexane) droplet on the fiber membrane in acidic water (pH 3) at 0 s (left) and after 12 h (right); (e) reversible water wettability of the as-prepared membrane between superhydrophobicity and superhydrophilicity; (f) reversible oil wettability of the as-prepared membrane between superoleophilicity and underwater superoleophobicity.

($A_{6.10-6.80}$) and CH_3O- ($A_{3.55-3.65}$). Thus, the calculated weight percent of P4VP is 51.0%, and M_n of $PMMA_{82}$-*b*-$P4VP_{80}$ is 16650 g/mol.

In addition to the ^1H NMR measurements, the results of gel permeation chromatography (GPC) before and after chain extension further verify the successful synthesis of the copolymer $PMMA_{82}$-*b*-$P4VP_{80}$ (Figure 1b). The GPC trace of $PMMA_{82}$-Cl (red lines) with M_n = 9200 g/mol moves toward the high-molecular-weight direction with M_n = 18800 g/mol (green lines). These results agree with those obtained by ^1H NMR. Furthermore, the narrow molar-mass dispersities of $PMMA_{82}$-Cl (M_w/M_n = 1.17) and $PMMA_{82}$-*b*-$P4VP_{80}$ (M_w/M_n = 1.28) indicate that the polymerization is well controlled and the resulting block copolymer has a relatively uniform property, which will benefit its application. On the basis of the obtained results, the volume fraction of P4VP calculated by the known densities of PMMA (1.18 g/cm^3) and P4VP (1.11 g/cm^3) is 0.53.[37]

3.2. Preparation and Characterization of the Fiber Membrane. Industrial stainless meshes with knitted steel strands are semipermeable barriers. Stainless steel meshes endowed with special water or oil wettability through surface functionalization can be used for oil/water separation.[38−43] Therefore, a smart fiber membrane was prepared by depositing pH-responsive copolymer fibers on a round steel mesh with an area of 23.7 cm^2. The fabrication process is described in Figure 2a. Parts b and c of Figure 2 show the SEM images of the steel meshes. The connected metal wires of the initial mesh were clearly visible, and the average size of the square-shaped pores was approximately 45 μm (Figure 2b). After electrospinning, the mesh was covered by a dense layer of entangled fibers, but bead and beads-on-string structures did not appear on the surface (Figure 2c). The highly magnified image in Figure 2c reveals that the fiber had a smooth surface with an average diameter of approximately 2.5 μm. The highly dense layer of entangled fibers leads to the formation of a 3D macroporous network structure, which facilitates the improvement of the liquid permeation rate across the membrane because of the decreased mass-transfer resistance.

3.3. Switchable Wettability of the Fiber Membrane. The P4VP block is a weak polybase with a pK_a of 4.5. The wettability of P4VP-based copolymer films can be altered at different pH media as a consequence of the protonation and deprotonation of pyridyl groups.[44−47] The other block, PMMA, is hydrophilic and underwater oleophilic.[48] Additionally, the geometrical structure of the surface has a significant influence on the surface wettability. To probe the special wettability of the as-prepared pH-responsive block copolymer fiber-coated membrane, the CAs of the membrane surface were initially measured in air. Figure 3a shows that, at the initial state, a nearly spherical water droplet with a CA of 152° formed on the membrane surface. Importantly, the water droplet gradually reduced in size as a result of evaporation; however, its spherical shape remained unchanged after 20 min, indicating the stable superhydrophobicity of the as-prepared membrane. The oil contact angle (OCA) measurements obtained with the use of an *n*-hexane droplet illustrate that the oil droplet penetrated into the membrane as soon as it came into contact with the surface, indicating the superoleophilicity of the membrane in air (Figure 3b).

Interestingly, the as-prepared fiber membrane displayed superhydrophobicity despite both the PMMA and deprotonated P4VP blocks having intrinsic CAs of less than 90°.[48] A rough structure is a key consideration in the construction of a superhydrophobic surface. In this study, the superhydrophobicity of the as-prepared fiber membrane was assumed to be caused by its 3D porous network structure and could be theoretically described by the C−B model.[30] More specifically, air trapped in the high-density micropores on the surfaces substantially reduced the contact area between water and the membrane and contributed to the high water repellency of the membrane surface. Additionally, the previous literature

DOI: 10.1021/acsami.5b04146
ACS Appl. Mater. Interfaces 2015, 7, 19643−19650

demonstrated the possibility of designing nonwetting surfaces for a given liquid, even if the same contacting liquid easily wets smooth surfaces made from the same material. Tuteja et al.[26] fabricated superoleophobic fiber mats using oleophilic materials as early as 2007. Overall, the unexpected high water repellency of the as-prepared membrane was rationalized by the rough surface containing an "air cushion" introduced by the 3D porous network structure of the fibers.

By contrast, the high affinity of the as-prepared membrane to oil in air was mainly caused by the low surface tension of oil (commonly lower than 30 mN/m)[49] and the surface feature of the membrane. In this study, the as-prepared block copolymer consisted of a PMMA block and a P4VP block with respective surface energies of 38.5 and 50.0 mJ/m^2 in air.[50−52] Therefore, the surface enrichment of the oleophilic block copolymer endowed the as-prepared membrane with oleophilicity. In addition, the oil-wetting behavior was further improved by the 3D macroporous structure of the fibers, resulting in the superoleophilic surface of the as-prepared membrane.

However, the wettability of the as-prepared membrane toward oil and water switched from superhydrophobicity/superoleophilicity to superhydrophilicity/underwater superoleophobicity after being saturated with pH 3 water. As shown in Figure 3c, the water droplet wet the surface gradually and spread over the membrane within approximately 100 s (in our experiment, the membrane was slightly dried under a nitrogen flow to monitor the wetting process). In pH 3 water, the oil droplet (*n*-hexane) formed a sphere with an OCA of 152° on the membrane surface (Figure 3d, left). Such oil repellency in acidic water was retained even after 12 h of immersion in the water (Figure 3d, right). In the present case, the weak polybase P4VP became protonated and the electrostatic repulsion between the pyridyl groups caused the P4VP segments to have an extended conformation. With the protonated P4VP blocks stretching out, the imbibition of water into the textures is promoted, and the air trapped in the pores of the fiber membrane is gradually replaced by water, ultimately leading to the superhydrophilicity of the surface.[46,47]

When the membrane was rinsed with large amounts of neutral water (pH 7), P4VP became deprotonated and returned to the collapsed state. The initial wettability of the fiber membrane was easily recovered. The microphase separation between the blocks on the surface and in the inner area of the fibers will be beneficial for the change in the P4VP chain conformation. Importantly, the switching of water wettability between superhydrophobicity and superhydrophilicity and oil wettability between superoleophilicity and underwater superoleophobicity can be repeated several times with a slight fluctuation in the responsiveness of the fiber membrane, as presented in parts e and f of Figure 3, respectively. A detailed discussion on the oil wettability in water is presented in the following section.

3.4. Underwater Oil Wettability of the Fiber Membrane. Aside from the wetting behavior of the surface in air, the underwater oil wetting behavior is important in oil/water separation.[53] The oil wettability of the as-prepared membrane was evaluated in aqueous media with different pH values. As can be seen in Figure 4a, when the fiber membrane was immersed in pH 3 water, the oil droplet (*n*-hexane) did not wet the membrane but instead formed a sphere with an OCA of 152° on the surface, demonstrating the underwater superoleophobicity of the membrane. A droplet with a sliding angle of less than 5° on the surface could roll away easily, indicating

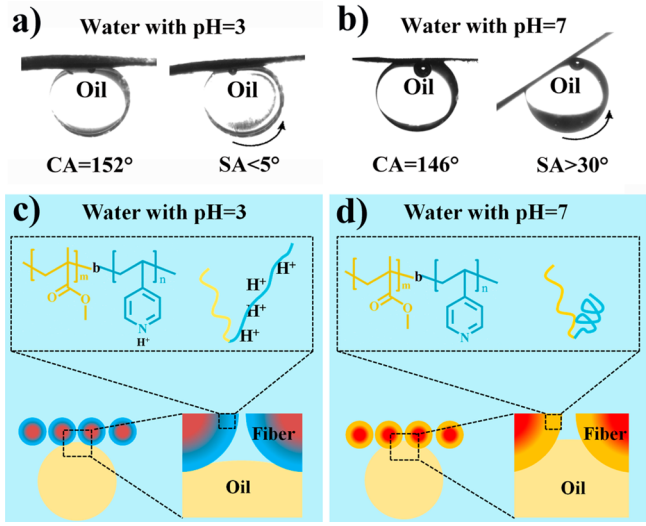

Figure 4. Oil wettability of the as-prepared fiber membrane in aqueous media with different pH values: (a) images of an oil (*n*-hexane) droplet on the fiber membrane in acidic water (pH 3) with an OCA of ∼152° (left) and a sliding angle of ∼4° (right); (b) images of an oil (*n*-hexane) droplet on the as-prepared membrane in neutral water (pH 7) with an OCA of ∼146° in a horizontal state (left) and a tilted state (right); (c and d) schematic description of the oil wetting behavior on the fiber membrane surface in pH 3 and 7 water, respectively.

that the as-prepared membrane has low oil adhesion in acidic water (Figure 4a, right). In comparison, when the fiber membrane was immersed in neutral water (pH 7), the OCA only slightly decreased to 146°, as shown in Figure 4b (left). The membrane did not display underwater pH-switchable oil wettability. However, the adhesive force between the oil droplet and the membrane surface exhibited an apparent pH-responsive change. The oil droplet always adhered to the membrane even if the surface moves from horizontal to a tilted state with an inclination angle of 30° (Figure 4b, right).

In the underwater environment, when the membrane came into contact with acidic water (pH 3), the protonated P4VP chains with an extended conformation were enriched on the membrane surface. As a consequence, the block copolymer structure connecting the two chemically different polymers at a point will facilitate chain extension on the base in microphase separation. The protonated P4VP on the exterior of the membrane was hydrophilic, and the water molecules with high oil repellency were trapped in the porous structure of the fiber membrane, leading to a composite oil/water/solid interface. As in the C−B model, the air trapped under the water caused the superhydrophobicity of the rough surface.[30] The composite oil/water/solid interface here created a surface with underwater superoleophobicity and low oil adhesion. The underwater oleophobic protonated P4VP blocks on the exterior of the membrane prevented contact between the oil droplet and the surface, thereby also leading to the low-oil-adhesive surface (Figure 4c). For the membrane in neutral water, although the deprotonated P4VP chains were in the collapsed state, they could not repel the water trapped in the porous structure of the fiber because of their moderate hydrophilicity. At the same time, the strong interaction between the oleophilic PMMA blocks and the oil droplets resulted in high adhesion of oil to the oleophobic surface (Figure 4d).

3.5. Controllable Oil/Water Separation. The two switchable wettability states (superhydrophobicity/superoleo-

DOI: 10.1021/acsami.5b04146
ACS Appl. Mater. Interfaces 2015, 7, 19643−19650

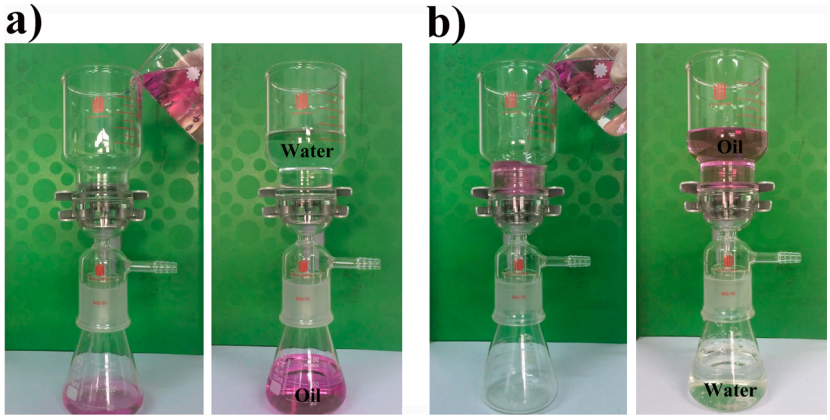

Figure 5. pH-controllable oil/water separation device: (a) Oil (*n*-hexane is colored with iodine) passed through the membrane, whereas water remained in the upper glass apparatus (right). (b) If the membrane was wetted with acidic water (pH 3) before separation, water could selectively permeate through the membrane, while oil could not (right).

philicity and superhydrophilicity/underwater superoleophobicity) of the as-prepared fiber membrane prove its potential in separating water−oil or water−organic solvent mixtures. As a proof of concept, a simple separation device, which is illustrated in Figure 5, was constructed. The as-prepared membrane was fixed between two glass apparatuses with flange connection, with a conical flask placed at the bottom as the container. When 200 mL of a layered mixture of water and oil (*n*-hexane colored with iodine) at a 1/1 volume ratio was poured directly into the upper glass apparatus, the oil immediately permeated through the membrane, whereas the water was retained (Movie SI-1 and Figure 5a). By contrast, if the as-prepared membrane was first saturated with acidic water (pH 3) without subsequent drying, the opposite effect was realized under the same conditions: water selectively passed through the membrane this time (Movie SI-2 and Figure 5b). Subsequently, the membrane was rinsed with neutral water and dried under a nitrogen flow, and the membrane reverted to the initial separation effect easily: oil permeated through and water was repelled.

To provide a better understanding of the pH-controllable oil/water mixture separation mechanism of the fiber membrane, Figure 6a models the microscopic water and oil wetting states of the fiber membrane during the separation process. At the initial state, the membrane was superhydrophobic and superoleophilic. When the oil/water mixture was poured onto the membrane, oil spread quickly on the fiber membrane, and the porous structure of the fiber membrane was filled with oil; consequently, the access of water was effectively blocked because of the high water repellency of nonpolar molecules (oil and deprotonated P4VP). Thus, oil passed through the fiber membrane, whereas water stayed on the membrane surface.

After separation, the membrane was dried under a nitrogen flow and rinsed with pH 3 water. The residual oil in the pores of the membrane could be partly removed by mechanical force. When the membrane was immersed in pH 3 water, the pyridyl groups of P4VP became protonated and stretched to the surface of the fiber gradually. The hydrophilic and oil-repellent protonated P4VP imbibes water into the textures, and oil and air trapped in the pores of the fiber membrane would gradually be replaced by water. The membrane surface ultimately acquired a superhydrophilic property. Unlike in the wettability study, no subsequent drying treatment was performed on the membrane after saturating it with pH 3 water. Thus, the membrane exhibited high oil repellency because of the trapped

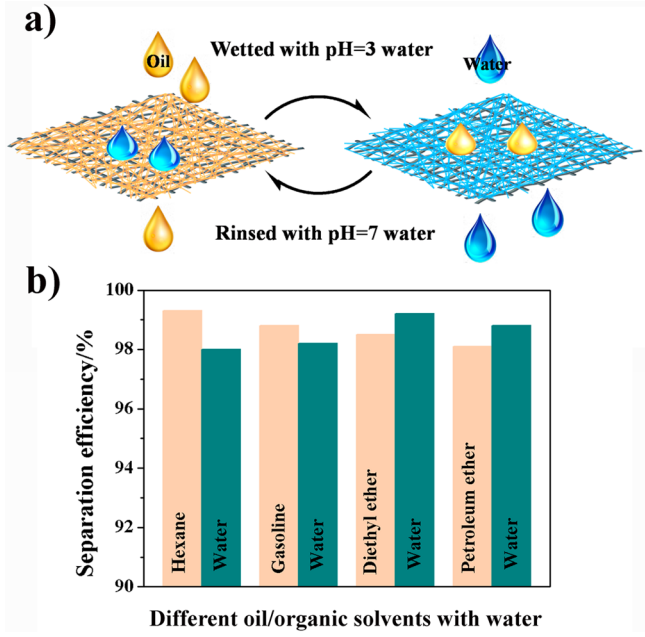

Figure 6. (a) Schematic diagrams of pH-switchable oil/water separation. In the initial state, oil passed through the membrane, whereas water stayed on the membrane (left); in the case of the membrane first fully wetted by pH 3 water, water selectively passed through, whereas oil was repelled (right). (b) Oil/organic solvent separation efficiency (dry state) and water separation efficiency (after wetted with pH 3 water) of four different mixtures. The separation efficiency was determined by comparing the weight of oil or water before and after separation.

water molecules in the voids between fibers. When an oil/water mixture was poured onto the membrane, water selectively passed through, whereas oil was repelled because of the macroporous network structure, which induced the stable underwater superoleophobicity of the fiber membrane. The prior saturation of the membrane with pH 3 water ensured the success and efficiency of the separation. Furthermore, the ultralow oil adhesion in pH 3 water of the membrane protected it from being fouled by oil during the separation; thus, the membrane exhibited an excellent oil-fouling repellency.[53]

Within the scope of the study, the as-prepared membrane exhibited excellent separation performance and recyclability. However, more details need to be considered in practical

DOI: 10.1021/acsami.5b04146
ACS Appl. Mater. Interfaces 2015, 7, 19643−19650

application. When the membrane is used for continuous separation, H^+ ions contained in the membrane will be gradually taken away by the passing neutral water, and consequently the pyridyl groups of P4VP will deprotonate and collapse. How then can the membrane sustain continuous separation? To this problem, a study about the underwater oil wetting behavior of the membrane revealed that, even in neutral water, the membrane still maintained a water-retention capacity because of the moderate hydrophilicity of deprotonated P4VP and PMMA. Therefore, the constantly water-saturated membrane allowed water to continuously pass through, whereas the oil was repelled. Unfortunately, the oil-fouling repellency of the membrane would be reduced by an increase in oil adhesion, and the flux and separation efficiency of the membrane would be negatively affected to some extent.

In addition, other oils, such as petroleum ether, diethyl ether, and gasoline, were mixed with water for further study; all of the oil/water mixtures were layered. All of the separation processes were driven solely by gravity and exhibited similar separation behaviors: the liquid passed through the membrane quickly because of the macroporous network structure of the fiber. The excellent separation efficiencies of the fiber membrane for different oil/water mixtures are described in Figure 6b. This versatile smart membrane with switchable wetting states for oil and water exhibits significant potential in the on-demand separation of oil/water mixtures. More importantly, the fiber membrane can maintain its 3D porous surface structure and exhibits excellent switchable wettability even after numerous cycles of the separation process (see Figure S1 in the Supporting Information). The recyclable property of the as-prepared fiber membrane well-matches the requirements of practical applications of oil/water separation.

4. CONCLUSION

In summary, a smart fiber membrane with two switchable wetting states (superhydrophobicity/superoleophilicity and superhydrophilicity/underwater superoleophobicity) was fabricated by depositing of pH-responsive copolymer fibers on a stainless steel mesh through electrospinning. The cost-effective precursor block copolymer PMMA-*b*-P4VP was synthesized using copper(0)-mediated RDRP. The as-prepared fiber membrane has accomplished on-demand oil/water separation using gravity alone by switching the pH of the medium. Initially, oil selectively passes through the membrane, whereas water remains. The separation process is reversed after wetting the membrane with acidic water (pH 3). Both separations exhibit high efficiency and flux that is attributed to the porous fiber structure of the membrane. More importantly, the fiber membrane can maintain its 3D porous surface structure and exhibit excellent switchable wettability after numerous cycles of the separation process. Therefore, this cost-effective, easily mass-produced, and recyclable smart fiber membrane is suitable for large-scale oil/water separation and has significant potential in practical applications, such as water purification and oil recovery.

■ ASSOCIATED CONTENT

Supporting Information

The Supporting Information is available free of charge on the ACS Publications website at DOI: 10.1021/acsami.5b04146.

Additional information about the SEM image of the as-prepared fiber membrane after numerous cycles of the separation processes and detailed characterizations (PDF)

Movie SI-1, video of pH-responsive controllable oil/water separation (AVI)

Movie SI-2, video of pH-responsive controllable oil/water separation (AVI)

■ AUTHOR INFORMATION

Corresponding Author

*E-mail: luozh@sjtu.edu.cn. Tel.: +86-21-54745602. Fax: +86-21-54745602.

Notes

The authors declare no competing financial interest.

■ ACKNOWLEDGMENTS

The authors thank the National Natural Science Foundation of China (Grant 21276213), the Research Fund for the Doctoral Program of Higher Education (Grant 20130073110077), and the National High Technology Research and Development Program of China (Grant 2013AA032302) for supporting this work.

■ REFERENCES

(1) Shannon, M. A.; Bohn, P. W.; Elimelech, M.; Georgiadis, J. G.; Marinas, B. J.; Mayes, A. M. Science and Technology for Water Purification in the Coming Decades. *Nature* **2008**, *452*, 301−310.

(2) Gao, C. R.; Sun, Z. X.; Li, K.; Chen, Y. N.; Cao, Y. Z.; Zhang, S. Y.; Feng, L. Integrated Oil Separation and Water Purification by a Double-layer TiO_2-Based Mesh. *Energy Environ. Sci.* **2013**, *6*, 1147−1151.

(3) Nguyen, D. D.; Tai, N.-H.; Lee, S.-B.; Kuo, W.-S. Superhydrophobic and Superoleophilic Properties of Graphene-Based Sponges Fabricated Using a Facile Dip Coating Method. *Energy Environ. Sci.* **2012**, *5*, 7908−7912.

(4) Chu, Z. L.; Feng, Y. J.; Seeger, S. Oil/Water Separation with Selective Superantiwetting/Superwetting Surface Materials. *Angew. Chem., Int. Ed.* **2015**, *54*, 2328−2338.

(5) Feng, L.; Zhang, Z. Y.; Mai, Z. H.; Ma, Y. M.; Liu, B. Q.; Jiang, L.; Zhu, D. B. A Super-Hydrophobic and Super-Oleophilic Coating Mesh Film for the Separation of Oil and Water. *Angew. Chem., Int. Ed.* **2004**, *43*, 2012−2014.

(6) Zhang, W. B.; Shi, Z.; Zhang, F.; Liu, X.; Jin, J.; Jiang, L. Superhydrophobic and Superoleophilic PVDF Membranes for Effective Separation of Water-in-Oil Emulsions with High Flux. *Adv. Mater.* **2013**, *25*, 2071−2085.

(7) Zhang, W. B.; Zhu, Y. Z.; Liu, X.; Wang, D.; Li, J. Y.; Jiang, L.; Jin, J. Salt-Induced Fabrication of Superhydrophilic and Underwater Superoleophobic PAA-g-PVDF Membranes for Effective Separation of Oil-in-Water Emulsions. *Angew. Chem., Int. Ed.* **2014**, *53*, 856−860.

(8) Kota, A.; Kwon, G.; Choi, W.; Mabry, J.; Tuteja, A. Hygro-Responsive Membranes for Effective Oil-Water Separation. *Nat. Commun.* **2012**, *3*, 1025−1029.

(9) Cao, Y. Z.; Liu, N.; Fu, C. K.; Li, K.; Tao, L.; Feng, L.; Wei, Y. Thermo and pH Dual-Responsive Materials for Controllable Oil/Water Separation. *ACS Appl. Mater. Interfaces* **2014**, *6*, 2026−2030.

(10) Xue, B. L.; Gao, L. C.; Hou, Y. P.; Liu, Z. W.; Jiang, L. Temperature Controlled Water/Oil Wettability of a Surface Fabricated by a Block Copolymer: Application as a Dual Water/Oil On-Off Switch. *Adv. Mater.* **2013**, *25*, 273−277.

(11) Tian, D. L.; Zhang, X. F.; Tian, Y.; Wu, Y.; Wang, X.; Zhai, J.; Jiang, L. Photo-Induced Water-Oil Separation Based on Switchable Superhydrophobicity-Superhydrophilicity and Underwater Superoleophobicity of the Aligned ZnO Nanorod Array-Coated Mesh Films. *J. Mater. Chem.* **2012**, *22*, 19652−19657.

DOI: 10.1021/acsami.5b04146
ACS Appl. Mater. Interfaces 2015, 7, 19643−19650

(12) Kwon, G.; Kota, A.; Li, Y. X.; Sohani, A.; Mabry, J. M.; Tuteja, A. On-Demand Separation of Oil-Water mixtures. *Adv. Mater.* **2012**, *24*, 3666−3671.
(13) Cheng, Z. J.; Du, M.; Fu, K. W.; Zhang, N. Q.; Sun, K. N. pH Controllable Water Permeation through a Nanostructured Copper Mesh Film. *ACS Appl. Mater. Interfaces* **2012**, *4*, 5826−5832.
(14) Cheng, Z. J.; Wang, J. W.; Lai, H.; Du, Y.; Hou, R.; Li, C.; Zhang, N. Q.; Sun, K. pH-Controllable On-Demand Oil/Water Separation on the Switchable Superhydrophobic/Superhydrophilic and Underwater Low-Adhesive Superoleophobic Copper Mesh Film. *Langmuir* **2015**, *31*, 1393−1399.
(15) Ju, G. N.; Cheng, M. J.; Shi, F. A pH-Responsive Smart Surface for the Continuous Separation of Oil/Water/Oil Ternary Mixtures. *NPG Asia Mater.* **2014**, *6*, e111.
(16) Xue, Z.; Cao, Y.; Liu, N.; Feng, L.; Jiang, L. Special Wettable Materials for Oil/Water Separation. *J. Mater. Chem. A* **2014**, *2*, 2445−2460.
(17) Wang, B.; Liang, W.; Guo, Z.; Liu, W. Biomimetic Super-lyophobic and Super-lyophilic Materials Applied for Oil/Water Separation: A New Strategy Beyond Nature. *Chem. Soc. Rev.* **2015**, *44*, 336−361.
(18) Zhang, L. B.; Zhang, Z. H.; Wang, P. Smart Surfaces with Switchable Superoleophilicity and Superoleophobicity in Squeous Media: Toward Controllable Oil/Water separation. *NPG Asia Mater.* **2012**, *4*, e8.
(19) Percec, V.; Guliashvili, T.; Ladislaw, J. S.; Wistrand, A.; Stjerndahl, A.; Sienkowska, M. J.; Monteiro, M. J.; Sahoo, S. Ultrafast Synthesis of Ultrahigh Molar Mass Polymers by Metal-Catalyzed Living Radical Polymerization of Acrylates, Methacrylates, and Vinyl Chloride Mediated by SET at 25 °C. *J. Am. Chem. Soc.* **2006**, *128*, 14156−14165.
(20) Zhou, Y.-N.; Luo, Z.-H. Copper(0)-Mediated Reversible-Deactivation Radical Polymerization: Kinetics Insight and Experimental Study. *Macromolecules* **2014**, *47*, 6218−6229.
(21) Xia, F.; Zhu, Y.; Feng, L.; Jiang, L. Smart Responsive Surfaces Switching Reversibly between Super-hydrophobicity and Super-hydrophilicity. *Soft Matter* **2009**, *5*, 275−281.
(22) Xin, B. W.; Hao, J. C. Reversibly Switchable Wettability. *Chem. Soc. Rev.* **2010**, *39*, 769−782.
(23) Zhou, Y.-N.; Li, J.-J.; Zhang, Q.; Luo, Z.-H. Light-Responsive Smart Surface with Controllable Wettability and Excellent Stability. *Langmuir* **2014**, *30*, 12236−12242.
(24) Zhou, Y.-N.; Li, J.-J.; Zhang, Q.; Luo, Z.-H. A Novel Fluorinated Polymeric Product for Photoreversibly Switchable Hydrophobic Surface. *AIChE J.* **2014**, *60*, 4211−4221.
(25) Liu, M.; Wang, S.; Wei, Z.; Song, Y.; Jiang, L. Bioinspired Design of a Superoleophobic and Low Adhesive Water/Solid Interface. *Adv. Mater.* **2009**, *21*, 665−669.
(26) Tuteja, A.; Choi, W.; Ma, M.; Mabry, J. M.; Mazzella, S. A.; Rutledge, G. C.; McKinley, G. H.; Cohen, R. E. Designing Superoleophobic Surfaces. *Science* **2007**, *318*, 1618−1622.
(27) Tuteja, A.; Choi, W.; Mabry, J. M.; McKinley, G. H.; Cohen, R. E. Robust Omniphobic Surfaces. *Proc. Natl. Acad. Sci. U. S. A.* **2008**, *105*, 18200−18205.
(28) Zhao, H.; Law, K.-Y.; Sambhy, V. Fabrication, Surface Properties, and Origin of Superoleophobicity for a Model Textured Surface. *Langmuir* **2011**, *27*, 5927−5935.
(29) Wenzel, R. N. Resistance of Solid Surfaces to Wetting by Water. *Ind. Eng. Chem.* **1936**, *28*, 988−994.
(30) Cassie, A. B. D.; Baxter, S. Wettability of Porous Surfaces. *Trans. Faraday Soc.* **1944**, *40*, 546−551.
(31) Ramakrishna, S.; Fujihara, K.; Teo, W. E.; Yong, T.; Ma, Z.; Ramaseshan, R. Electrospun Nanofibers: Solving Global Issues. *Mater. Today* **2006**, *9*, 40−50.
(32) Wang, X.; Ding, B.; Sun, G.; Wang, M.; Yu, J. Electro-Spinning/Netting: A Strategy for the Fabrication of Three-Dimensional Polymer Nano-fiber/Nets. *Prog. Mater. Sci.* **2013**, *58*, 1173−1243.
(33) Lee, M. W.; An, S.; Latthe, S. S.; Lee, C.; Hong, S.; Yoon, S. S. Electrospun Polystyrene Nanofiber Membrane with Superhydrophobicity and Superoleophilicity for Selective Separation of Water and Low Viscous Oil. *ACS Appl. Mater. Interfaces* **2013**, *5*, 10597−10604.
(34) Che, H.; Huo, M.; Peng, L.; Fang, T.; Liu, N.; Feng, L.; Wei, Y.; Yuan, J. CO_2-Responsive Nanofibrous Membranes with Switchable Oil/Water Wettability. *Angew. Chem., Int. Ed.* **2015**, *54*, 8934−8938.
(35) Tsarevsky, N. V.; Braunecker, W. A.; Brooks, S. J.; Matyjaszewski, K. Rational Selection of Initiating/Catalytic Systems for the Copper-Mediated Atom Transfer Radical Polymerization of Basic Monomers in Protic Media: ATRP of 4-Vinylpyridine. *Macromolecules* **2006**, *39*, 6817−6824.
(36) Vidts, K. R. M.; Du Prez, F. E. Design of Water-Soluble Block Copolymers Containing Poly(4-vinylpyridine) by Atom Transfer Radical Polymerization. *Eur. Polym. J.* **2006**, *42*, 43−50.
(37) *Polymer Data Handbook*; Mark, J. E., Ed.; Oxford University Press: New York, 1999.
(38) Wang, F. J.; Lei, S.; Xue, M. S.; Ou, J. F.; Li, W. In Situ Separation and Collection of Oil from Water Surface via a Novel Superoleophilic and Superhydrophobic Oil Containment Boom. *Langmuir* **2014**, *30*, 1281−1289.
(39) Wang, L. F.; Yang, S. Y.; Wang, J.; Wang, C. F.; Chen, L. Fabrication of Superhydrophobic TPU Film for Oil-Water Separation Based on Electrospinning Route. *Mater. Lett.* **2011**, *65*, 869−872.
(40) Jing, B. X.; Wang, H. T.; Lin, K. − Y.; McGinn, P. J.; Na, C. Z.; Zhu, Y. X. A Facile Method to Functionalize Engineering Solid Membrane Supports for Rapid and Efficient Oil-Water Separation. *Polymer* **2013**, *54*, 5771−5778.
(41) Yang, Y. Z.; Li, H. D.; Cheng, S. H.; Zou, G. T.; Wang, C. X.; Lin, Q. Robust Diamond Meshes with Unique Wettability Properties. *Chem. Commun.* **2014**, *50*, 2900−2903.
(42) Crick, C. R.; Gibbins, J. A.; Parkin, I. P. Superhydrophobic Polymer-Coated Copper-Mesh; Membranes for Highly Efficient Oil-Water Separation. *J. Mater. Chem. A* **2013**, *1*, 5943−5948.
(43) Wang, B.; Guo, Z. G. pH-Responsive Bidirectional Oil-Water Separation Material. *Chem. Commun.* **2013**, *49*, 9416−9418.
(44) Zhang, W. Q.; Shi, L. Q.; Ma, R. J.; An, Y. L.; Xu, Y. L.; Wu, K. Micellization of Thermo- and pH-Responsive Triblock Copolymer of Poly(ethylene glycol)-*b*-Poly(4-vinylpyridine)-*b*-Poly(N-isopropylacrylamide). *Macromolecules* **2005**, *38*, 8850−8852.
(45) Mendrek, S.; Mendrek, A.; Adler, H.-J.; Dworak, A.; Kuckling, D. Synthesis and Characterization of pH Sensitive Poly(glycidol)-*b*-Poly(4-vinylpyridine) Block Copolymers. *J. Polym. Sci., Part A: Polym. Chem.* **2009**, *47*, 1782−1794.
(46) Escalé, P.; Rubatat, L.; Derail, C.; Save, M.; Billon, L. pH Sensitive Hierarchically Self-Organized Bioinspired Films. *Macromol. Rapid Commun.* **2011**, *32*, 1072−1076.
(47) Geng, Z.; Guan, S.; Jiang, H.-M.; Gao, L.-C.; Liu, Z.-W.; Jiang, L. pH-Sensitive Wettability Induced by Topological and Chemical Transition on the Self Sssembled Surface of Block Copolymer. *Chin. J. Polym. Sci.* **2014**, *32*, 92−97.
(48) Ma, Y.; Cao, X.; Feng, X.; Ma, Y.; Zou, H. Fabrication of Super-Hydrophobic Film from PMMA with Intrinsic Water Contact Angle Below 90°. *Polymer* **2007**, *48*, 7455.
(49) Xue, Z. X.; Liu, M. J.; Jiang. Lei. Recent Developments in Polymeric Superoleophobic Surfaces. *J. Polym. Sci., Part B: Polym. Phys.* **2012**, *50*, 1209−1224.
(50) Kwok, D. Y.; Leung, A.; Lam, C. N. C.; Li, A.; Wu, R.; Neumann, A. W. Low-Rate Dynamic Contact Angles on Poly(methyl methacrylate) and the Determination of Solid Surface Tensions. *J. Colloid Interface Sci.* **1998**, *206*, 44−51.
(51) Wu, S. Surface and Interfacial Tensions of Polymer Melts. II. Poly(methyl methacrylate), Poly(n-butyl methacrylate) and Polystyrene. *J. Phys. Chem.* **1970**, *74*, 632−638.
(52) Sohn, B. H.; Seo, B. W.; Yoo, S. I.; Zin, W. C. Sluggish Development of Parallel Lamellae at the Strongly Interacting Interface in Thin Films of Symmetric Diblock Copolymers. *Langmuir* **2002**, *18*, 10505−10508.
(53) Zheng, X.; Guo, Z. Y.; Tian, D. L.; Zhang, X. F.; Li, W. X.; Jiang, L. Underwater Self-Cleaning Scaly Fabric Membrane for Oily Water Separation. *ACS Appl. Mater. Interfaces* **2015**, *7*, 4336−4343.

DOI: 10.1021/acsami.5b04146
ACS Appl. Mater. Interfaces 2015, 7, 19643−19650